JOURNAL OF VIROLOGY, Sept. 1996, p. 5954–5961 Vol. 70, No. 9
0022-538X/96/$04.00+0

Cleavage Site Mutations in the Encephalomyocarditis Virus P3 Region Lethally Abrogate the Normal Processing Cascade

DAVID J. HALL AND ANN C. PALMENBERG*

Institute for Molecular Virology and Department of Animal Health & Biomedical Sciences, University of Wisconsin—Madison, Madison, Wisconsin 53706

Received 22 January 1996/Accepted 17 May 1996

Site-specific mutations within the proteinase 3C-dependent P3 region cleavage sequences of encephalomyocarditis virus have been constructed. The mutations altered the normal QG cleavage site dipeptide pairs of the 2C/3A, 3A/3B, 3B/3C, and 3C/3D junctions into QV, QC, QF, QY, and RG sequences. When translated in vitro in the context of full-length viral polyproteins, all mutations blocked endogenous 3C-mediated processing at their engineered sites and produced stable forms of the expected viral P3 precursors that were also resistant to cleavage by exogenously added recombinant 3C. Relative to wild-type viral sequences, each mutant form of P3 had a somewhat different ability to mediate overall polyprotein processing. Mutations at the 2C/3A, 3A/3B, and 3B/3C sites, for example, were generally less impaired than 3C/3D mutations, when the cleavage reactions were quantitated with cotranslated L-P1-2A precursors. A notable exception was mutant 3B3C$_{(QG\rightarrow RG)}$, which proved far less active than sibling mutants 3B3C$_{(QG\rightarrow QF)}$ and 3B3C$_{(QG\rightarrow QV)}$, a finding that possibly implicates this segment in the proper folding of an active 3C. When transfected into HeLa cells, all mutant sequences were lethal, presumably because of the reduced L-P1-2A processing levels or reduced RNA synthesis capacity. However, when specifically tested for the latter activity, all mutations except those at the 3C/3D cleavage site were indeed able to initiate and perpetuate viral RNA replication in transfected cells, albeit to RNA accumulation levels lower than those produced by wild-type sequences. The transfection effects could be mimicked with cell-free synthesized proteins, in that translation samples containing locked 3CD polymerase precursors were catalytically inactive in poly(A)-oligo(U)-dependent assays, while all other mutant processing samples initiated detectable RNA synthesis. Surprisingly, not only did the 3B/3C mutant sequences prove capable of directing RNA synthesis, but the viral RNA thus synthesized could be immunolabeled and precipitated with 3C-specific monoclonal antibody reagents, indicating an unexpected covalent attachment of the proteinase to the RNA product whenever this cleavage site was blocked.

Picornavirus RNA genomes encode a large polyprotein which is proteolytically processed in cotranslational and post-translational reactions by several self-encoded reactive centers. The majority of cleavages are catalyzed by one specific proteinase, 3C, an unusual cysteine-reactive, chymotrypsin-like sequence located in the carboxyl third of the polyprotein. During translation, 3C is synthesized in an enzymatically active form, and even while still part of the nascent polyprotein, it rapidly and efficiently catalyzes an ordered series of monomolecular and bimolecular scissions within its parental molecule to release mature viral proteins and precursor combinations.

The consensus 3C cleavage sites in most picornavirus polyproteins are at Gln-Gly dipeptide pairs, but not all conforming viral sequences are always cleaved, and in many virus strains, alternative combinations like Gln-Ser, Gln-Ala, Glu-Gly, or Glu-Ser occur at the natural sites (6). Experiments with partially purified 3C enzymes and synthetic or mutated substrates sometimes show a substrate repertoire even broader than that evident from natural sequences. With encephalomyocarditis virus (EMCV) from the genus *Cardiovirus*, the 3C-catalyzed cleavages occur at Gln-Gly, Gln-Ser, and Glu-Ser dipeptide sequences (6), but this enzyme will also recognize and process other mutated dipeptides that generally contain either Gln or Glu in the first (P1) position and are followed by a small aliphatic amino acid, i.e., Gly, Ser, Ala, or Cys, in the second (P1′) position. Larger hydrophobic (Val or Ile), charged (Glu), branched (Thr), or aromatic (Tyr) residues have proven not to be viable substrates for EMCV 3C when substituted into the P1′ positions of the polyprotein cleavage sites (19, 20).

Within the natural 3C-catalyzed cleavage cascade, each released viral protein or polyprotein precursor is presumed to contribute in a vital way to the replication and fecundity of the virus. The 3C enzyme and its P3 region precursors typify this assertion, and in reality, these proteins should probably be viewed as a group of enzymatic species (3C, 3ABC, 3CD, and 3ABCD) rather than a unique proteolytic entity. In enteroviruses and rhinoviruses, for example, the 3CD precursor is the catalytic unit vested with the cleavage of most capsid precursor locations (26). The 3CD additionally participates in plus-strand RNA synthesis, by mediating a virus-specific binding interaction with the 5′ region of the genome (3, 16). For EMCV, the capsid region cleavages are generally carried out by released 3C, although 3ABC, 3CD, and 3ABCD precursors also have demonstrable *trans* activity with these same substrates (19) and it is assumed that these precursors play additional catalytic roles in the replication cycle, as they do for the enteroviruses and rhinoviruses.

Few studies have detailed the importance of 3C-containing precursors in the replication cycle or the timely release of these precursors into this cycle (10, 11, 15). Given that EMCV polyproteins translated in cell extracts undergo a processing cascade closely mimicking that of the infected cells, we have now been able to use this system in controlled assessments of multiple P3 region cleavage site defects. Engineered mutations

* Corresponding author. Mailing address: Department of Animal Health & Biomedical Sciences, 1655 Linden Dr., Madison, WI 53706. Phone: (608) 262-7519. Fax: (608) 262-7420. Electronic mail address: Palmenberg@bioinformatics.bocklabs.wisc.edu.

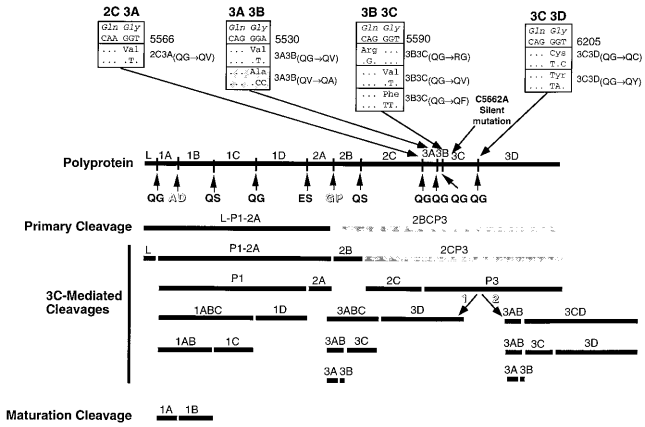

FIG. 1. EMCV processing map. The polyprotein of EMCV-R, its processing sites, and its cleavage products are depicted. Sites cleaved by proteinase 3C are in boldface. The primary cleavage (2A/2B) and maturation cleavage (1A/1B) sites are shadowed. Gray proteins are hypothetical precursors formed only when natural sites are mutated. Two alternative P3 paths (1 and 2) are depicted. The recombinant substitutions created for this study are identified, as is the silent (marker) mutation (C5662A) that tagged all recombinant sequences. The QV-to-QA change at 3A/3B is a natural reversion. Base numbering is that of EMCV-R.

preventing 3C-dependent cleavage at the 2C/3A, 3A/3B, 3B/3C, and 3C/3D processing sites were created and tested in vitro for their consequent blocks in the processing cascade and effects on polymerase activity. The mutations were also characterized in vivo within the context of full-length genomic sequences for defects in RNA synthesis, genetic stability, and subsequent infectivity. The data confirm the essential indispensability and preferred order of the natural processing cascade and point to a fine balance between 3C protein precursors and polyprotein products in establishment of an infectious cycle.

MATERIALS AND METHODS

Recombinant cDNA and RNA. Standard recombinant methods were used (4, 23). The sequences of EMCV-R (GenBank accession no. M81861), infectious cDNA plasmid pEC_4, and translational plasmid pE5P3 have been described previously (5, 19). The *Sac*II-*Sal*I fragment from pEC_4 was inserted into the multiple cloning site of pBS-SK+ to create mutagenesis vector pEP2P3. Two-primer site-directed mutagenesis (Transformer kit; Clontech) was then used to create multiple substitutions in the EMCV P3 region proteolytic cleavage sequences, as summarized in Fig. 1. The mutated cDNAs were reintroduced into pEC_4 by replacement of the *Sac*II-*Sal*I fragment and into pE5P3 by replacement of a *Ppu*MI-*Mlu*I fragment. To produce viral RNA transcripts, pE5P3 (digested with *Bam*HI) or pEC_4 (digested with *Sal*I) cDNAs and their related mutant sequences were added to reaction mixtures with T7 polymerase (Bethesda Research Laboratories) and [α-^{32}P]UTP as described previously (9). After DNase I treatment and phenol-chloroform extraction, the samples were precipitated with ethanol and monitored for radiolabel by scintillation counting after adsorption to Whatman DE81 filters (23).

Progeny virus growth. Confluent HeLa cell monolayers (6×10^6 cells on 60-mm-diameter plates) were washed with a solution of 2 ml of phosphate-buffered saline (PBS; 0.1 M phosphate, 100 mM NaCl [pH 7.2]) and then 2 ml of Hanks' balanced salt solution. RNA transcripts from pEC_4 plasmids (1 to 10 μl) were mixed with Hank's balanced salt solution (240 μl), Transfectace (10 μl; Bethesda Research Laboratories), and RNasin (15 U; Promega) and then allowed to react with the monolayer for 30 min at 22°C. Medium A (2.5 ml) (22) was added, and resultant virus was allowed to undergo amplification. Alternatively, the monolayer was overlaid with P5 (2.5 ml) containing 0.8% agarose for plaque development (22). All infected or transfected plates were incubated at 37°C under 5% CO_2 for 24 h unless otherwise indicated. Mutant viral RNA was isolated from plaque picks by sodium dodecyl sulfate (SDS) and acid phenol extraction (9). The RNA was reverse transcribed with Moloney murine leukemia virus reverse transcriptase (Bethesda Research Laboratories), and the resulting cDNA was amplified in the region of interest by PCR with *Pfu* polymerase (Stratagene). The PCR fragments were precipitated with ethanol, resuspended, and fractionated on low-melting-point agarose gels and then purified by Wizard prep techniques (Promega) before sequencing (Sequenase; U.S. Biochemicals).

Viral RNA detection. Total cellular RNA was isolated from transfected HeLa cells with guanidine isothiocyanate (4), assayed for concentration by spectrophotometry at A_{260} and A_{280}, and size checked by agarose electrophoresis. Samples (10 μg) were denatured (65°C for 15 min) in 120 μl of a solution containing 65% formamide, 8% formaldehyde, 25 mM MOPS (morpholinepropanesulfonic acid; pH 7.0), 10 mM NaOAc, and 1 mM EDTA and then placed on ice before cold 20× SSC (2 volumes) (1× SSC is 0.15 M NaCl plus 0.015 M sodium citrate) was added.

For immunoprecipitations, anti-mengovirus 3C monoclonal antibody (0.1 μg of 6D10) was added to total cellular RNA (10 μg) and the two were reacted at 4°C for 30 min (6). Goat anti-mouse antibodies coupled to magnetic beads (Advanced Magnetics) were added (5 μl of suspension), and incubation was continued for 30 min at 4°C. The beads were isolated with a magnetic stand and washed three times with Nonidet P-40 buffer (25 mM Tris-Cl [pH 7.5], 5 mM $MgCl_2$, 1 mM EDTA, 1 mM dithiothreitol 0.1% Nonidet P-40). The immunocomplexes were solubilized and denatured with 100 μl of denaturing buffer (described above).

The mixture was transferred onto a Hybond-N membrane (Amersham) with a slot blotter (Hybri-slot manifold; Bethesda Research Laboratories), washed twice with 10× SSC (500 μl), air dried, and then irradiated (254 nm, 690,000 μJ/cm^2 [UV Stratalinker 1800; Stratagene]). The RNA-containing membrane was incubated with hybridization buffer (10 ml; 5× SSC, 50% formamide, 5× Denhardt's reagent, 10% dextran sulfate, 10 mg of sheared salmon sperm DNA per ml, 1% SDS) at 60°C for 3 h before [α-^{32}P]UTP-labeled viral RNA probe (120 ng; 10^8 dpm/μg) was added and the incubation was continued at 60°C for 12 h. The probe (T3 transcript of pEP2P3 cDNA, linearized with *Bgl*II) corresponded to EMCV minus-strand bases 6082 to 7730 (3D coding region). The membrane was washed twice (15 min; 60°C) with high-salt buffer (50 ml; 2× SSC–1% SDS) and twice (15 min; 60°C) with low-salt buffer (50 ml; 0.2× SSC–1% SDS) before radioactivity was localized and quantitated with a PhosphorImager using Imagequant software (Molecular Dynamics).

For Western (immunoblot) analyses, RNA samples were bonded to membranes as described above and then incubated (30 min; 22°C) with BLOTTO buffer (5% [wt/vol] nonfat dry milk–0.05% [wt/vol] Tween-20 in PBS) and rinsed twice in wash buffer (0.05% [wt/vol] Tween-20 in PBS) before anti-mengovirus 3C monoclonal antibody 6D10 at a 1:5,000 dilution was added (6) and the incubation was continued (1 h at 22°C). After two rinses with wash buffer, the membranes were incubated (1 h; 22°C) with horseradish peroxidase-conjugated anti-mouse antibody (1:2,000 dilution in BLOTTO buffer; Amersham) and rinsed twice in wash buffer and once in water and the bands were visualized by chemiluminescence (ECL kit; Amersham).

Cell-free assays. Viral RNA transcripts were analyzed for size and homogeneity by agarose electrophoresis and then added to cell-free translation reaction mixtures with rabbit reticulocyte extracts (at 50 μg/ml) as described previously (6). The extracts contained [^{35}S]methionine (1 μCi/μl) and were incubated with the RNA for 1 h at 30°C before the addition of RNase A and cycloheximide to 0.33 mg/ml. To test for viral polymerase activity, samples (5 μl) of translated extracts (without RNase A treatment) were added to polymerase reaction buffer {50 μl; 50 mM HEPES (*N*-2-hydroxyethylpiperazine-*N*′-2-ethanesulfonic acid; pH 8.0), 3 mM magnesium acetate (MgOAc), 10 mM dithiothreitol, 8 μM $ZnCl_2$, 20 μg of rifampin per ml, 0.67 μM UTP, 5 μg of poly(A), 2 μCi of [α-^{32}P]UTP, oligo(U)} and then incubated at 30°C for 1 h. Carrier tRNA (100 μg/ml in 20 mM sodium PP_i; Sigma) was added, and the reaction mixtures were made 20% in trichloroacetic acid. Precipitates were collected on Gelman filters (0.45-mm pore size), and radiolabel incorporation was monitored by scintillation counting.

RESULTS

P3 region processing. Site-specific mutations were introduced into the nucleotides encoding the polyprotein Gln-Gly pairs at the 3B/3C and 3C/3D cleavage junctions of EMCV cDNA (Fig. 1). The resultant sequences were translated in cell extracts from the context of RNAs containing the EMCV internal ribosomal entry site linked to the 3′ third of the viral genome (pE5P3). The P3 region polyprotein fragments were allowed to undergo processing in the presence or absence of exogenously added recombinant mengovirus 3C protease (rM3C). As expected, the unmutated *P3 precursor cleaved efficiently to yield 3CD, 3D, 3C, and *3AB even in the absence of exogenous protease (Fig. 2, lanes 1 and 2). Also as expected, replacement of the natural 3B/3C QG sequence with RG, QF, or QV prevented *P3 cleavage at this junction and gave rise to a *3ABC band and its reciprocal, 3D (lanes 3 to 8). The two 3C/3D mutations, QY and QC, showed prominent 3CD precursor bands (lanes 9 to 12), but the QC sequence, as previ-

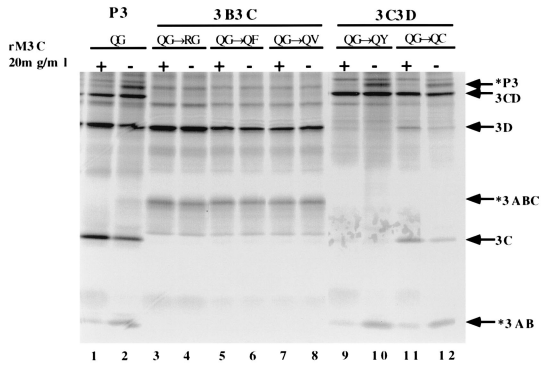

FIG. 2. Cell-free translation of P3 region RNA. Transcripts from pE5P3 containing the indicated mutations were translated in reticulocyte extracts (15 μl; 1 h at 30°C). Duplicate samples received 1 μl of H_2O (even-numbered lanes with minus signs) or 1 μl of recombinant rM3C (to 20 μg/ml; odd-numbered lanes with plus signs) and then further incubation (30°C for 1 h). Samples were made 10% in SDS, precipitated with acetone, fractionated on 5 to 20% acrylamide gradient gels (SDS-polyacrylamide gel electrophoresis), and visualized by autoradiography.

ously reported (19), was partially reactive at this site. The endogenous 3C reaction with this mutation was clearly enhanced when rM3C was added, and 3D and 3C products were stronger in these lanes (lane 11 and 12).

Polyprotein processing. The mutations described above, and two additional constructions at the 2C/3A (to QV) and 3A/3B (to QV) cleavage sites (Fig. 1), were transferred into full-length viral cDNAs (pEC_4). Again, each sequence was transcribed and then translated in cell extracts, with care taken to ensure that similar RNA concentrations were added to each reaction mixture. Each sample incorporated the same amount of radioactivity throughout the time course, and this was evidence that the various processing schemes did not affect general translation rates (data not shown). The processing patterns, however, were dramatically varied and dependent upon the type and location of each cleavage mutation (Fig. 3). Gel patterns from samples taken sequentially during the translation reactions (30 to 60 min) and subsequently during processing reactions (2 to 6 h) showed a strong, normal cleavage cascade, dependent upon the endogenous 3C sequences in the wild-type RNA samples (Fig. 3A). The $3A3B_{(QG\rightarrow QV)}$ profile was similar to that of the wild type (data not shown), as was the $3B3C_{(QG\rightarrow QF)}$ profile (Fig. 3E), but the $2C3A_{(QG\rightarrow QF)}$ and $3B3C_{(QG\rightarrow QV)}$ polyproteins were processed more slowly and less completely (Fig. 3B and C, respectively). Least active were the $3B3C_{(QG\rightarrow RG)}$ (Fig. 3D), $3C3D_{(QG\rightarrow QC)}$ (Fig. 3F), and $3C3D_{(QG\rightarrow QY)}$ (data not shown) samples, which produced few mature viral proteins from their respective polyprotein precursors.

To better quantitate what was happening with regard to the catalytic activity of each mutant P3 form, all gels from the above-described experiment were digitized by phosphorimaging. The data conversion allowed direct comparison of precursor and product profiles for the individual sequences and at individual sites (Fig. 4). In a cardiovirus polyprotein, the L-P1-2A precursor is cotranslationally separated from the nascent strand by a unique autocatalytic mechanism (18). It is only subsequent to this reaction that 3C, translated from the carboxyl portion of the polyprotein, is synthesized and begins its reactions. The independence of L-P1-2A release, relative to 3C synthesis, and the fact that four 3C-catalyzed sites are located within this precursor made the specific processing of L-P1-2A an excellent comparative assay for 3C-mediated activity.

In the normal processing cascade the four reactions appear stepwise, first at L/P12A, then at P1/2A, followed by 1ABC/1D, and finally at 1AB/1C (20). Data from the wild-type translations clearly follow this pattern (Fig. 3 and 4). The L protein appeared within 35 min of reaction and was followed at 45 min by 2A. Longer reactions were required to see 1AB and 1D. The $3A3B_{(QG\rightarrow QV)}$ sequence was most similar to the wild type in both the rate and the extent of precursor-to-product conversion. The profiles of $2C3A_{(QG\rightarrow QV)}$, $3B3C_{(QG\rightarrow QV)}$, and $3B3C_{(QG\rightarrow QF)}$ were marginally delayed compared with and generally less robust than those of the wild-type sequences, a phenomenon especially apparent during the last cascade step, 1AB/1C. Figure 4 (panel 1C) shows retarded release of 1C for both of these 3B3C mutants, with $3B3C_{(QG\rightarrow QV)}$ being slower, and virtually no release from the $2C3A_{(QG\rightarrow QV)}$ samples. Oddly, the remaining 3B3C mutant containing the RG sequence was much less efficient overall than its sibling, same-site sequences. After 3 h of reaction with $3B3C_{(QG\rightarrow RG)}$, most of the L-P1-2A precursor was still untouched, and of the P12A and P1 that was produced, almost none was cleaved further. The 1ABC, 1D, and 1C quantitations from this sequence were virtually baseline. Only the 3C3D mutations were less effective P1 region processors. Neither 3C3D sequence, i.e., neither QC nor QY, was capable of sustained reaction with any of the capsid precursors. Although L, 2A, and a small amount of 1ABC were eventually released, this form of locked 3C precursor (3CD) was evidently not a preferred protease species for P1 processing.

When full-length polyproteins were processed, the cleavage profiles of the P2 and P3 region precursors were always more difficult to characterize precisely, especially when certain sites

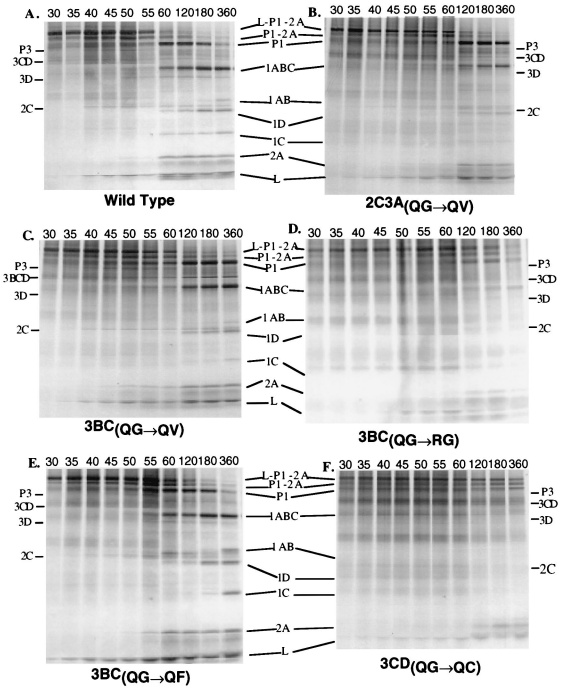

FIG. 3. Cell-free translation of genomic RNA. Transcripts from pEC_4 containing the indicated mutations were translated in reticulocyte extracts. At the indicated times (in minutes), aliquots were removed and made 10% in SDS. After 60 min, translation was stopped and incubation was continued for up to 6 h. Equivalent extract volumes for each time point were fractionated on 5 to 20% acrylamide gradient gels (SDS-polyacrylamide gel electrophoresis), and the bands were visualized by autoradiography.

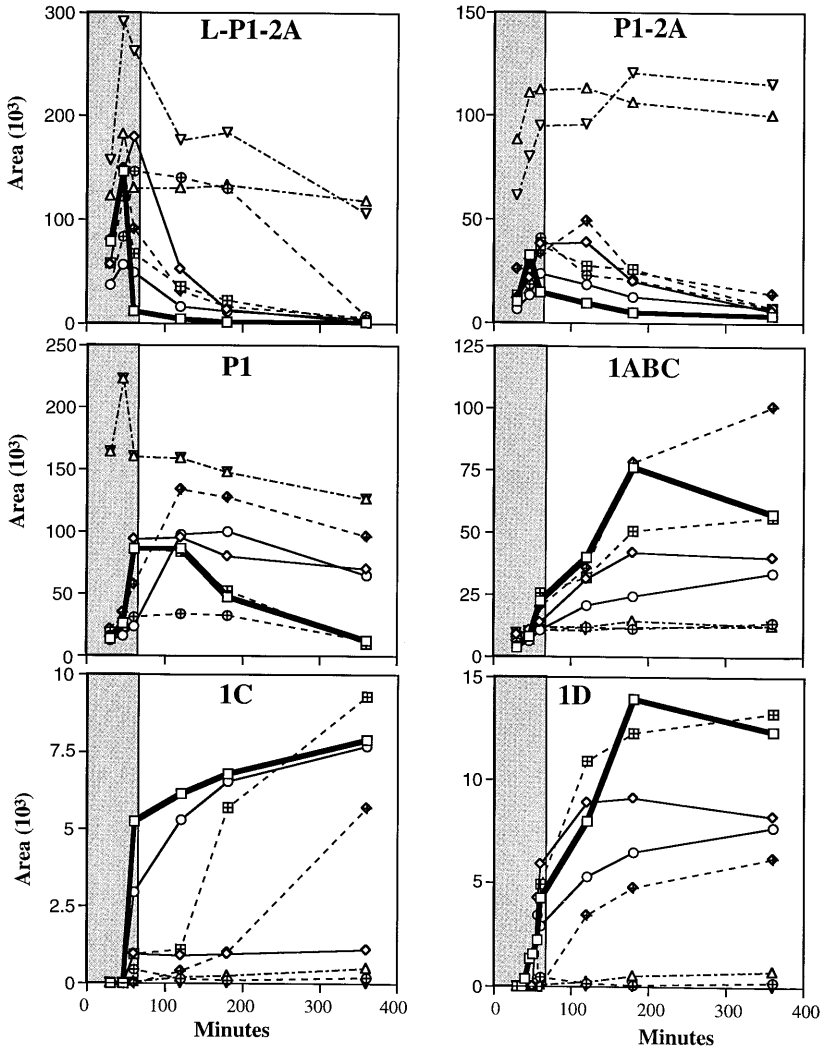

FIG. 4. Quantitation of processing reactions. The gels depicted in Fig. 3 were analyzed by phosphorimaging, and the P1 region bands were quantitated with IPlabgel (Signal Analytics) software. The panels indicate relative peak areas (in pixels) for particular proteins as plotted against the incubation times of the translation samples. The wild-type profile is emphasized. The shaded areas are incubation times during which translation was active. □, wild type; ○, $3A3B_{(Q/G\rightarrow Q/V)}$; ⊞, $3B3C_{(Q/G\rightarrow Q/F)}$; △, $3C3D_{(Q/G\rightarrow Q/C)}$; ◇, $2C3A_{(Q/G\rightarrow Q/V)}$; ⊕, $3B3C_{(Q/G\rightarrow R/G)}$; ◈, $3B3C_{(Q/G\rightarrow Q/V)}$; ▽, $3C3D_{(Q/G\rightarrow Q/Y)}$.

were blocked mutagenically. Still, there were trends evident from the different tested sequences that generally mimicked the patterns translated from smaller RNAs (Fig. 2). Release of P3 (faint) and appearance of 2C coincided at around 40 min of reaction in the wild-type, $3B3C_{(QG\rightarrow QV)}$, and $3B3C_{(QG\rightarrow QF)}$ samples. At 60 min and beyond, most of this P3 was processed and its constituent proteins (e.g., 3D) became visible. Elements of this pattern varied from mutant to mutant. Most notably, an unusual 3BCD precursor was prominent in the $3B3C_{(QG\rightarrow QV)}$ lanes but not with $3B3C_{(QG\rightarrow QF)}$. The $3B3C_{(QG\rightarrow RG)}$ and 3C3D mutants were difficult to document with any P3 reactivity except for the putative 3ABC bands in the $3B3C_{(QG\rightarrow RG)}$ lanes at mid-time course. Most material remained in larger precursor forms, indicating that these cascades, apart from the primary cleavage reactions, were significantly disrupted by the incorporated mutations.

Infectivity of mutant sequences. EMCV RNA and transcripts from pEC_4 cDNA are highly infectious in HeLa cells. After transfection, large plaques appeared within 24 h at a specific infectivity of about 10^5 PFU/μg (Table 1). When the seven mutated RNAs were equivalently transfected, only the $2C3A_{(QG\rightarrow QV)}$ sample produced any direct plaques, and these were of much lower specific infectivity and of variable size (Table 1). Only blind passage of transfected cell material eventually forced the appearance of plaques from the other sequences. Of exception were the two mutations at the 3C/3D cleavage site. No amount of additional passage ever produced viable virus from these RNAs.

Suspecting that all the mutant sequences were actually lethal and that the few plaques obtained were revertants, we repeated the transfections with special tagged RNAs containing C-5662 to A (C5662A), a silent substitution in the third position of the 25th codon (Pro) of the 3C coding region, in addition to the cleavage site mutations. The genetic tag allowed discrimination between true revertant sequences and wild-type (virus) contamination. For each of the 3B3C mutants, 12 spontaneous large-plaque viruses were picked and purified (four each from three independent transfections). Sequencing of the 3B/3C site, as well as the entire 3C gene, showed each of these viruses to be wild type at every base,

TABLE 1. Infectivities of mutants with cleavage site mutations[a]

Mutant	Infectivity (PFU/μg)	Sequenced reversion (amino acid change)	No. of isolates	Plaque size	C5662A present
Wild type	$\sim 10^5$			Large	No
$2C3A_{(QG\rightarrow QV)}$	$<10^2$	T5265G (V→G)	6	Large	Yes
$3A3B_{(QG\rightarrow QV)}$	<1	T5529G (V→G)	6	Large	Yes
		TA5529–30CC (V→A)[b]	6	Small	Yes
$3B3C_{(QG\rightarrow RG)}$	<1	G5586A (R→Q)	12	Large	Yes
$3B3C_{(QG\rightarrow QF)}$	<1	TT5588–89GG (F→G)	12	Large	Yes
$3B3C_{(QG\rightarrow QV)}$	<1	T5589G (V→G)	12	Large	Yes
$3C3D_{(QG\rightarrow QC)}$	<1		0		
$3C3D_{(QG\rightarrow QY)}$	<1		0		

[a] HeLa cell monolayers were transfected with 5 to 500 ng of genome-length RNA transcripts. Mutant $2C3A_{(QG\rightarrow QV)}$ RNA transcripts produced plaques after 48 h. With other mutants plaques were observed after transfected HeLa cells were lysed (after 24 to 72 h) and replated onto fresh cells. All putative revertant viruses were plaque purified (twice) before amplification to verify the stability of their plaque phenotypes and their genetic homogeneity. The presence of silent mutation C5662A confirmed that recovered revertants were not the result of wild-type EMCV contamination.

[b] TA5529–30CC, T5529C plus A5530C.

except 5662, at which they all maintained the genetic tag. The direct reversion of $3B3C_{(QG\rightarrow QF)}$ requires genetic fixation of two transversion substitutions (TT to GG), and both were found in all 12 sampled isolates. The variable plaques observed upon transfection with $2C3A_{(QG\rightarrow QV)}$ RNA invariably stabilized with large-plaque phenotypes when picked and passaged. Six such isolates from $2C3A_{(QG\rightarrow QV)}$ and six from $3A3B_{(QG\rightarrow QV)}$ were also sequenced (three each from two independent transfections) and found again to contain direct same-site mutations at the respective locations of the original mutations.

Six additional $3A3B_{(QG\rightarrow QV)}$ plaques had uniformly smaller-plaque phenotypes relative to the wild type or to the other revertants. These were each sequenced with a new QA alteration that fixed a transition (T to C) and a silent mutation (A to C) at the second and third positions of the Val cleavage site codon. Interestingly, QA is not a natural 3C cleavage dipeptide within EMCV. Previous engineered mutations, however, within the capsid region, had shown this sequence to be recognized by the protease (19). To ensure that the viable phenotype of QA at the 3A/3B site was legitimate, a pEC_4 cDNA containing the $3A3B_{(QG\rightarrow QA)}$ changes was reconstructed. Transcription and transfection gave the same small-plaque phenotype as was observed for the natural revertants (data not shown).

RNA accumulation after transfection. The lethality of all tested P3 mutations and the absence of reversion from either locked 3C3D sequence suggested that RNA synthesis pathways, in addition to the processing pathways, might be severely compromised in mutant transfected cells. Accordingly, HeLa cells were transfected with equivalent amounts of the various RNAs, and at intervals over 24 h, total cellular (and viral) RNA was collected. Quantitated samples were blotted onto membranes and then probed with radiolabeled RNA complementary to the viral 3D coding region (Fig. 5A). The increase in signal after wild-type RNA transfection indicated vigorous viral RNA synthesis, but against this benchmark, the accumulation of mutant RNAs was severely retarded. Specifically, neither of the mutant 3C3D sequences gave any hint of detectable signal, except for the samples immediately after transfection (0-h time point). Presumably this signal arose from input RNA, because within 4 h the activity had diminished to the background level. Reverse transcription and PCR were likewise unable to detect any evidence of minus-strand RNA accumulation in the 3C3D samples (data not shown), and it was clear that these particular mutations had lethally abrogated replication by preventing RNA synthesis.

The other mutants faired slightly better. By the 8-h time point, the remaining five sequences had accumulated about 20% of the RNA levels of the wild type. Thereafter, the three 3B3C sequences showed marginal increases in RNA levels and $3A3B_{(QG\rightarrow QV)}$ had a moderate increase, to an endpoint about 30% of that of the wild type. The $2C3A_{(QG\rightarrow QV)}$ sequence was the most active of all tested mutants, an observation consistent with its higher specific infectivity in the viability assays. From these data it could not be concluded, however, whether the relative vigor of 2C3A was intrinsic to the QV mutation itself or just reflective of a higher spontaneous reversion frequency.

Cell-free polymerase activity. One hypothesis for the failure of cleavage site mutants to synthesize RNA after transfection was that 3D or consequent 3D precursors generated in cells were defective in polymerase activity. To test this assumption, full-length mutant RNAs were translated in cell extracts, and the protein was allowed to undergo processing for 2 h and then tested for primer-dependent polymerase activity (Fig. 5B). The assays were standardized with recombinant mengovirus 3D (lane 4). Radiolabel incorporation required the presence of enzyme (lane 1), oligo(U) (lane 2), and poly(A) (lane 3). Protein from the translation of wild-type RNA (lane 5) or

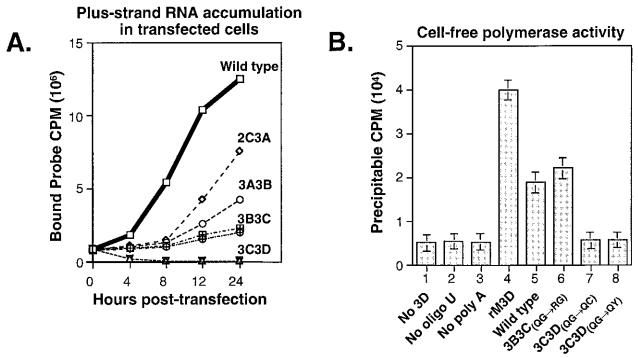

FIG. 5. RNA synthesis activity. RNA transcripts (0.5 μg) from pEC_4 containing the indicated mutations were transfected into HeLa cells. (A) At the indicated the times posttransfection, total cellular RNA was harvested, blotted onto membranes, and then probed with ^{32}P-labeled viral RNA. The signals were quantitated by phosphorimaging. Plotted values are averages for triplicate samples. (B) pEC_4-derived transcripts were translated in reticulocyte extracts for 1 h and then the protein was allowed to undergo processing for 2 h as described in the legend to Fig. 3. Poly(A)-oligo(U)-dependent polymerase activity in the extracts was assayed as described in Materials and Methods. The plotted values are averages from three independent translation reactions (duplicate samples for each). Standard deviations are indicated. rM3D, recombinant mengovirus 3D.

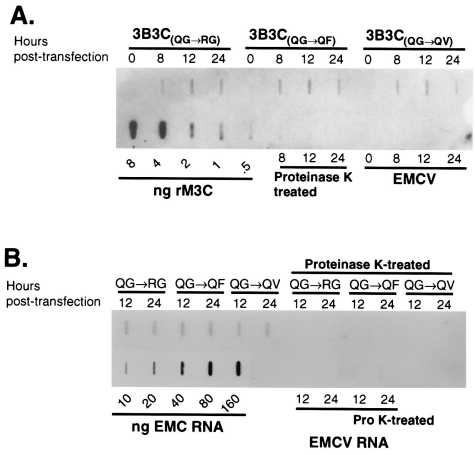

FIG. 6. Immunoreactions with 3C. Total cellular RNA was isolated after transfection of HeLa cells with genomic transcripts of pEC_4 or the indicated mutant RNAs and then blotted onto membranes. Equivalent samples of $3B3C_{(QG\rightarrow QV)}$ RNAs were treated with proteinase K (Pro K) before blotting. Additional slots contained quantities of purified rM3C. (A) Membranes (5 μg of RNA per slot) were probed by Western analysis with monoclonal antibody 6D10 (6). The bands were visualized by chemiluminescence, recorded on film, and then scanned by computer imaging. (B) The extracted RNA samples (5 μg) described above were immunoprecipitated with 6D10, blotted onto membranes, and then probed with ^{32}P-labeled viral RNA fragments. Control samples contained defined amounts of virion EC_4 RNA. The signals were quantitated by phosphorimaging. EMC, EMCV.

$3B3C_{(QG\rightarrow RG)}$ RNA (lane 6) showed significant activity, indicating that the 3D sequences translated from these RNAs could elongate a primed template. In contrast, samples from the $3C3D_{(QG\rightarrow QY)}$ and $3C3D_{(QG\rightarrow QC)}$ translations were totally inactive (lanes 7 and 8). The results confirm that the 3C3D mutations imposed a significant barrier to RNA synthesis. In the absence of substantial processing at this cleavage site, even the partially reactive QC sequence was unable to carry out a polymerase activity.

3C association with RNA. Protein 3B has been proposed to act as a synthesis primer that is essential for the polymerase-dependent initiation that occurs during picornavirus replication. This protein is normally found covalently attached by a phosphodiester bond to the 5′ ends of all viral plus and minus RNA strands (1, 21). Because of their processing defects, four of our mutants, with alterations at the 3A/3B and 3B/3C sites, were incapable of 3B release. Yet RNA accumulation assays and isolation of viable revertants suggested that these sequences were undergoing detectable RNA replication and, by inference, 3B addition. To test this possibility, cellular RNAs from mutant and wild-type transfected HeLa cells were blotted onto membranes and then probed with a monospecific antibody raised against rM3C and known to cross-react with 3C from EMCV (Fig. 6A). A surprising time-dependent signal was associated with samples from each 3B3C mutant but not with the wild-type samples. The signal was eliminated by proteinase K treatment prior to blotting, indicating that it arose from protein and not a fortuitous RNA interaction. Calibration blots with rM3C, combined with viral RNA estimations from the accumulation assays, gave molar amounts of about 2.1 pmol of 3C to 1.9 pmol of RNA in samples from the 24-h time points. Thus, the ratios between the detected 3C signal and viral RNA estimations were roughly 1:1. RNAs isolated after 2C3A and 3A3B transfections had no detectable signals (data not shown), presumably because their 3B/3C and 3C/3D cleavage release sites were native and active.

To confirm that the 3B3C antibody signals were also dependent upon viral RNA, the 12- and 24-h transfected RNA samples were immunoprecipitated with antibody. Material that precipitated was blotted onto a membrane and then probed with radiolabeled RNA fragments complementary to the viral 3D coding region (Fig. 6B). Again, all 3B3C mutant samples gave positive signals that were eliminated when the RNAs were pretreated with proteinase K before immunoprecipitation. Wild-type RNA-transfected samples were not reactive in this assay unless they were directly blotted without immunoprecipitation. Clearly, during the mutant 3B3C RNA transfections, some form of antibody-recognizable 3C protein, presumably 3BC, had become strongly associated with the viral RNAs, allowing specific immunoprecipitation by 3C antibody.

DISCUSSION

To date, numerous genetic studies, primarily with poliovirus, have tried to clarify the biological functions of the P2 and P3 nonstructural proteins in the picornavirus replication cycle. Early reports established that protein 3C is a proteinase, protein 3D is an RNA polymerase, and protein 3B or VPg is attached to both viral plus strands and viral minus strands during the process of RNA synthesis (1, 14, 21). The problem of identifying all properties intrinsic to these and other proteins, such as 2B, 2C, and 3A, has been complicated by suspicions that the rate and order with which each is proteolytically released from the polyprotein or from its subsequent cleavage products are intricately linked to the observation of activity. With poliovirus 3C for example, the proteinase sequences not only control the monomolecular and bimolecular polyprotein cleavage but also, as part of a 3CD complex in the presence of 3AB, play a vital role in RNA replication by enabling a binding activity with the 5′-most nucleotides of the viral RNA (2, 3, 8, 25). The proteolytic activity of poliovirus 3C is also somehow modulated by its precursor form, in that 3CD but not mature 3C is an apparent requirement for capsid processing at particular cleavage sequences (12, 26).

The present study focused on the catalytic consequences of 3C precursors in cardioviruses. As a counterpoint to the poliovirus data, previous results from cell-free expression of EMCV P3 proteins have shown that multiple forms of the 3C proteinase could effectively process exogenously added L-P1-2A capsid substrates (19). In particular, mature 3C was the preferred catalytic entity for the processing of L-P1-2A (6). Moreover, a lower concentration of 3CD relative to 3D in EMCV-infected cells seemed inconsistent with the poliovirus analog's requirement for 3CD during RNA synthesis (6, 8). Instead of reexamining mature viral products, we looked more closely at the region's precursors by mutating the 3C-dependent cleavage sites at four P3 locations and testing processing and replication consequences in the context of genomic RNAs. Site-specific mutations at the QG sequences between 2C and 3A, 3A and 3B, 3B and 3C, and 3C and 3D were created within cDNAs and shown to be effective at preventing *cis* and *trans* cleavage. The exceptional sequence, QC, at the 3C/3D junction was expected to provide partial reactivity (19). What weren't expected were the severe, long-range consequences for both cleavage and RNA synthesis that were imparted by every tested mutation. Each substitution proved lethal, including the QC at 3C/3D. Only same-site viable revertants could be isolated, but not for every mutation. Despite this lethality, definite phenotypic trends, as measured in processing and replication assays, were apparent in the severity of the mutations, and moreover these phenotypes correlated with the location of the

altered sites as they moved progressively towards the carboxyl end of the polyprotein.

Fusion of the 3C3D sequences was the most detrimental. Mutation to QC or QY disrupted processing throughout the polyprotein. Only the primary reaction at 2A/2B, which cleaved before 3CD was synthesized, remained entirely functional. Most sites within the L-P1-2A, P2, and P3, although unmutated, were never properly processed. This effect was surprising in view of observations that 3C/3D is usually cleaved as one of the last polyprotein processing steps. Presumably, the inability to process at 3C/3D was somehow anticipated at multiple higher levels of the cascade, and alternative pathways or alternative forms of 3C were unable to compensate significantly. Viral transcripts containing these mutations were unable to initiate detectable RNA accumulation upon transfection, and moreover, cell extracts that had translated these sequences did not participate in poly(A)-oligo(U)-dependent synthesis. The former observation suggests why no revertants were isolated from the 3C3D mutants, and the latter observation strongly indicates that complete 3D release from its precursors is a prerequisite to any polymerizing activity. Indeed, the analogous poliovirus 3CD also shows no polymerase activity (7, 17, 24). However, similar abrogating mutations at the poliovirus 3C/3D site, when tested in a full-length context, were capable of reverting to wild-type sequences (13). But for EMCV, the 3C/3D cleavage proved to be a linchpin reactivity for infectivity, and its rate and timed release during the processing cascade were the most essential among those of the tested polyprotein reactions.

Also thought to be essential was release of 3B (Vpg) before RNA synthesis. The correlate assumption that 3AB or 3BC would be an ineffective primer proved only partially true when tested with actual mutations. Preventing the release of mature 3C by substitution at the 3B/3C site had only a partial impact on the other processing steps. The QV and QF substitutions showed nearly wild-type cleavage activities in the L-P1-2A cycle, and with the exception of the 1AB/1C cleavage, which was inefficient relative to the wild type, both sequences completed the majority of the cascade at reasonable rates. However, the RG change at this same site had a very different profile. The $3B3C_{(QG\rightarrow RG)}$ pattern, like the 3C3D mutations, was disruptive to all regions of the polyprotein. Possibly, the incorporation of RG instead of QG caused a change in 3C structure or catalytic conformation within this precursor. As observed, a putatively misfolded 3C would process poorly in all regions of the polyprotein. Alternatively, it is also conceivable that an altered cleavage sequence in which the P1 rather than the P1′ residue was changed impinged on 3C catalysis by competitive substrate binding. Further tests for these hypotheses now require additional mutagenesis at the 3B/3C site.

Regardless of the processing mechanism, all 3B3C mutants were capable of low-level, albeit detectable, viral RNA synthesis after transfection. When probed with 3C-specific antibody, the proteinase, presumably as 3BC or 3ABC, was strongly associated with viral RNA. The signal was removed only with proteinase K treatment. To our knowledge, this is the first observation of a 3C precursor attached to viral RNA. Quantitative Western and Northern (RNA) analyses suggested that the proteinase and the RNA were equimolar, further implying that uridylation of VPg (3B) and initiation of RNA synthesis proceeded without 3B release. In cell-free samples, the RG mutant was as active as a wild-type sequence in poly(A)-oligo(U) assays, confirming again that 3C/3D cleavage, which is unaffected in this mutant, was probably the obligate step for polymerase activity.

Of all constructed sequences, $3A3B_{(QG\rightarrow QV)}$ was least disruptive of the processing cascade. The time course and banding pattern were essentially wild type. Since the 3A/3B site is rarely cleaved in cell extracts (19), this effect was consistent with expectations that 3C is unaffected by nearby abnormal substrates. Upon transfection, $3A3B_{(QG\rightarrow QV)}$ directed moderate RNA synthesis, indicating that viral replication was not dependent upon 3B release to initiate this process. Of course, the 3A3B mutation was still lethal, and only same-site revertants to QG or QA (a natural Theiler's murine encephalomyelitis virus sequence at this site) were isolated as plaques. But it remains unclear whether lethality was caused by reduced RNA synthesis or by some other untested VPg-dependent effect (perhaps packaging). An interest that we intend to pursue is the creation of antibody reagents specific to 3A, 3B, and 2C to confirm the presence of other uncleaved precursors at the ends of these RNAs.

Normally present among the most reactive of 3C substrates (10, 11), the last mutation at 2C/3A should have precluded P3 liberation and prevented further processing if the overall cascade proceeded sequentially. Instead, like the 3A3B mutation, the 2C/3A site was bypassed when mutated. Cell-free processing was similar to that of the wild type except for the final P1 step, in which 1AB/1C was unreactive, perhaps reflecting a preference for 3ABC proteinase at this site. In terms of infectivity and RNA synthesis, 2C3A was the most difficult mutant to characterize precisely, because all plaques quickly stabilized as direct same-site revertants, a phenomenon that may have caused or been the result of heightened RNA accumulation relative to the other mutations.

That mutants with each of the tested mutations, except that at the 3C/3D site, could replicate suggests that most P3 region precursors probably functioned in the RNA synthesis pathway as proteins larger than 3AB or 3CD (e.g., 3ABCD or 2C3ABCD). However, that none of the mutations was without phenotypic consequence also argues convincingly that in vivo nuances of sequence context and protein structure strongly influence the overall rates at which individual cleavage sites are selected and processed during natural viral infections and, moreover, that these parameters must play critical regulatory roles in the orderly release of viral proteins throughout the infectious cycle.

ACKNOWLEDGMENTS

This work was supported by National Institutes of Health (NIH) grant AI-17331 to A.C.P. and NIH training grant GM-07215 to D.J.H.

We thank Hernando Duque for the gift of recombinant mengovirus 3D and Carolyn Rinke and Wai-Ming Lee for valuable advice and assistance.

REFERENCES

1. **Ambros, V., and D. Baltimore.** 1978. Protein is linked to the 5′ end of poliovirus RNA by a phosphodiester linkage to tyrosine. J. Biol. Chem. **253:**5263–5266.
2. **Andino, R., G. E. Rieckhof, P. L. Achacoso, and D. Baltimore.** 1993. Poliovirus RNA synthesis utilizes an RNP complex formed around the 5′-end of viral RNA. EMBO J. **12:**3587–3598.
3. **Andino, R., G. E. Rieckhof, and D. Baltimore.** 1990. A functional ribonucleoprotein complex forms around the 5′ end of poliovirus RNA. Cell **63:**369–380.
4. **Ausubel, F., R. Brent, R. E. Kingston, D. D. Moore, J. G. Seidman, J. A. Smith, and K. Struhl.** 1993. Current protocols in molecular biology. John Wiley & Sons, Inc., New York.
5. **Hahn, H., and A. C. Palmenberg.** 1995. Encephalomyocarditis viruses with short poly(C) tracts are more virulent than their mengovirus counterparts. J. Virol. **69:**2697–2699.
6. **Hall, D. J., and A. C. Palmenberg.** Mengo virus 3C proteinase: recombinant expression, intergenus substrate cleavage and localization *in vivo*. Virus Genes, in press.
7. **Harris, K. S., S. R. Reddigari, M. J. H. Nicklin, T. Hammerle, and E. Wimmer.** 1992. Purification and characterization of poliovirus polypeptide

3CD, a proteinase and a precursor for RNA polymerase. J. Virol. **66:**7481–7489.
8. **Harris, K. S., W. Xiang, L. Alexander, A. V. Paul, W. S. Lane, and E. Wimmer.** 1994. Interaction of the poliovirus polypeptide 3CDpro with the 5′ and 3′ termini of the poliovirus genome: identification of viral and cellular cofactors necessary for efficient binding. J. Biol. Chem. **269:**27004–27014.
9. **Hoffman, M. A., and A. C. Palmenberg.** 1995. Mutational analysis of the J-K stem-loop region of the encephalomyocarditis virus IRES. J. Virol. **69:**4399–4406.
10. **Jackson, R. J.** 1986. A detailed kinetic analysis of the *in vitro* synthesis and processing of encephalomyocarditis virus products. Virology **149:**114–127.
11. **Jackson, R. J.** 1989. Comparison of encephalomyocarditis virus and poliovirus with respect to translation initiation and processing in vitro, p. 51–71. *In* B. L. Semler and E. Ehrenfeld (ed.), Molecular aspects of picornavirus infection and detection. American Society for Microbiology, Washington, D.C.
12. **Jore, J., B. de Geus, R. J. Jackson, P. H. Pouwels, and B. E. Engervalk.** 1988. Poliovirus protein 3CD is the active protease for processing of the precursor protein P1 *in vitro*. J. Gen. Virol. **69:**1627–1636.
13. **Kean, K. M., H. Agut, O. Fichot, E. Wimmer, and M. Girard.** 1988. A poliovirus mutant defective for self cleavage at the COOH-terminus of the 3C protease exhibits secondary processing defects. Virology **163:**330–340.
14. **Kitamura, N., C. J. Adler, P. G. Rothberg, J. Martinko, S. G. Nathenson, and E. Wimmer.** 1980. The genome-linked protein of picornaviruses. VII. Genetic mapping of poliovirus VPg by protein and RNA sequence studies. Cell **21:**295–302.
15. **Lawson, M. A., and B. L. Semler.** 1992. Alternate poliovirus nonstructural protein processing cascades generated by primary sites of 3C protease cleavage. Virology **191:**309–320.
16. **Molla, A., K. S. Harris, A. K. Paul, S. H. Shin, J. Mugavero, and E. Wimmer.** 1994. Stimulation of poliovirus proteinase 3C-related proteolysis by the genome-linked protein VPg and its precursor 3AB. J. Biol. Chem. **269:**27015–27020.
17. **Morrow, C. D., B. Warren, and M. R. Lentz.** 1987. Expression of enzymatically active poliovirus RNA-dependent RNA polymerase in *Escherichia coli*. Proc. Natl. Acad. Sci. USA **84:**6050–6054.
18. **Palmenberg, A. C., G. D. Parks, D. J. Hall, R. H. Ingraham, T. W. Seng, and P. V. Pallai.** 1992. Proteolytic processing of the cardioviral P2 region: 2A/2B cleavage in clone-derived precursors. Virology **190:**754–762.
19. **Parks, G. D., J. C. Baker, and A. C. Palmenberg.** 1989. Proteolytic cleavage of encephalomyocarditis virus capsid region substrates by precursors to the 3C enzyme. J. Virol. **63:**1054–1058.
20. **Parks, G. D., and A. C. Palmenberg.** 1987. Site-specific mutations at a picornavirus VP3/VP1 cleavage site disrupt in vitro processing and assembly of capsid precursors. J. Virol. **61:**3680–3687.
21. **Rothberg, P. G., T. J. R. Harris, A. Nomoto, and E. Wimmer.** 1978. O4-(5′-uridylyl) tyrosine is the bond between the genome-linked protein and the RNA of poliovirus. Proc. Natl. Acad. Sci. USA **75:**4868–4872.
22. **Rueckert, R. R., and M. A. Pallansch.** 1981. Preparation and characterization of encephalomyocarditis virus. Methods Enzymol. **78:**315–325.
23. **Sambrook, J., E. F. Fritsch, and T. Maniatis.** 1989. Molecular cloning: a laboratory manual, 2nd ed. Cold Spring Harbor Laboratory, Cold Spring Harbor, N.Y.
24. **Van Dyke, T. A., and J. B. Flanegan.** 1980. Identification of poliovirus polypeptide p63 as a soluble RNA-dependent RNA polymerase. J. Virol. **35:**732–740.
25. **Xiang, W., K. S. Harris, L. Alexander, and E. Wimmer.** 1995. Interaction between the 5′-terminal cloverleaf and 3AB/3CD of poliovirus is essential for RNA replication. J. Virol. **69:**3658–3667.
26. **Ypma-Wong, M. F., P. G. Dewalt, V. H. Johnson, J. G. Lamb, and B. L. Semler.** 1988. Protein 3CD is the major poliovirus proteinase responsible for cleavage of the P1 capsid precursor. Virology **166:**265–270.